

What to do when carbonate replaced water: *Carb*, the model for estimating the dose rate of carbonate-rich samples

Barbara Mauz¹ and Dirk Hoffmann²

¹School of Environmental Sciences, University of Liverpool, Jane Herdman Building, Liverpool L69 3GP, United Kingdom

²School of Geographical Sciences, University of Bristol, University Road, Bristol BS8 1SS United Kingdom

(Received 4 September 2014; in final form 21 November 2014)

Introduction

In 2008 we published a paper (Nathan and Mauz, 2008) where we described, calculated and modeled the impact of carbonate on the dose rate. Since then the software (called '*Carb*') has been employed in several studies (Mauz et al., 2009, 2012, 2013) resulting in a clear and unequivocal impact on the accuracy of the OSL ages which allowed to improve sedimentological models on the 100 ka Milankovitch time scale (Mauz et al., 2013). This increased the confidence that the dose-rate model is a reliable tool to correct for post-depositional chemical alterations involving carbonate.

Since publication, Nathan and Mauz, 2008 received some attention, but it failed to incentivise dose-rate modeling where it was - according to sample description in the relevant publications - certainly appropriate. We conclude that more attention needs to be drawn to this issue by (i) providing a clear and comprehensive description of the impact of carbonate on the dose rate and by (ii) making the code available to users.

When Nathan and Mauz (2008) was published, *Carb* suffered from two weaknesses: (1) correction of U-series secular disequilibrium caused by post-mortem U-uptake of mollusk shells was not possible and (2) interstitial carbonate was assumed to be inert while no data were available to (dis-)prove this.

With this short paper we wish to encourage users to appreciate (i) the importance of dose-deposition efficiency and its dependence on material properties and (ii) the significance of dose-rate change over time. We aim at removing doubts and misunderstandings about the impact of carbonate on dose rate, at explaining the code including its update, its assumptions and limitations and at providing instructions on how to use it.

For description of the underlying physics, in particular the infinite matrix concept, calculation of attenuation factors, determination of mass stopping powers and mass absorption coefficients, the reader

is referred to the original paper (Nathan and Mauz, 2008), to Guérin et al. (2012), Guérin and Mercier (2012) and, of course, to Aitken (1985) and references herein.

Carbonate and the cementation process

Cementation is the process which turns loose sediment into rock. It occurs in marine, lacustrine, fluvial and aeolian environments through new minerals (forming cements) being precipitated as a matrix in the pores between the primary sediment particles (i.e. detrital components). A cemented sediment is then composed of primary components (e.g., detrital quartz, feldspar, limestone particles), matrix (i.e. cement) and "empty" pore space (filled by water or air). Cement formation is caused by precipitation of calcium carbonate (CaCO₃) minerals from a pore fluid that is oversaturated with respect to a carbonate phase. The process of cementation and its timing depends largely on the pH and temperature of the water-sediment mixture, the availability of CO₂ from bacterial oxidation, permeability of the sediment and hydrodynamic conditions. The process of cementation can start during sedimentation (syn-sedimentary) or after sedimentation (burial). During burial dissolution, reprecipitation and recrystallisation of the carbonate mass can occur. These processes follow the relative thermodynamic stability of the carbonate minerals (e.g., calcite, aragonite) and the chemistry of the pore fluid with the end-point of the process being chemical stability.

The dose-rate correction factor

At the time of sedimentation of the detrital components the pore material is air and water. At $t=0$ which is the time when the pore material starts changing, carbonate precipitates in the existing pore space where it gradually replaces water or air. At $t=1$ the change ceased and the carbonate content is achieved as measured today (for details of this concept see Nathan and Mauz's Fig 3). When the

material of the pore space changes, so do the energy spectra of beta and gamma rays and the related energy absorption.

The relative energy absorption of the pore material (i.e. water, air, carbonate) compared to the primary sediment components is expressed by the correction factor x and was computed by Zimmerman (1971) as the effective ratio of mass stopping powers of water and aluminium for beta radiation and the effective ratio of mass absorption coefficients for gamma radiation. With $x=1$ detrital sediment components and pore material (matrix) absorb the same average amount of dose over a given radiation spectrum. Table 1 lists the correction factors in terms of the different ratios (carbonate/sediment and water/sediment) for beta radiation. The values demonstrate an increase of the dose to quartz deposition when water is replaced by carbonate (because "water absorbs more than its fair share"; Aitken, 1985, p. 69). They also show that the transition from water to carbonate becomes significant for the dose rate when the carbonate content exceeds around 20% of the total pore material.

	m_c/m_s			
m_w/m_s	0	0.04	0.20	1.00
0	-	0.99	0.99	0.99
0.04	1.19	1.09	1.03	1.00
0.20	1.20	1.09	1.09	1.02
1.00	1.19	1.18	1.15	1.09

Table 1. The correction factor x for beta radiation for water and carbonate to sediment mass ratios (m_s = sediment mass; m_c =carbonate mass; m_w = water mass). Values in italic are theoretical because they do not exist in nature. For details regarding radioactive elements see Nathan and Mauz (2008).

For beta radiation Zimmerman (1971) calculated $x=1.25$ for water. Our value is 1.19 in agreement with Guérin and Mercier (2012). The values of x decrease by up to 17% (i.e. from 1.19 to 0.99) when all water is replaced by carbonate. For gamma radiation the difference is around 11% when $x=1.14$ (Zimmerman, 1971) is used for water. Aitken and Xie (1990) computed $x=1.065$ and our analysis revealed 1.06-0.98 for K, Th and U in water using the same data as Aitken and Xie (1990) but excluding secondary electrons. But because secondary electrons play a role in gamma dose-rate absorption and because Guérin and Mercier (2012) found values between 1.19 and 1.13 using the Monte Carlo simulation software GEANT4, the original Zimmerman value is

still valid. Guérin and Mercier (2012) also show that for the energies considered (0.05-3 MeV) the x values increase with decreasing particle size with a trend towards a limiting value of 1.20 for particle sizes between 20-500 μm .

The activity of carbonate

Most sedimentary environments are a sink for radionuclides originating from detrital input. In addition to detrital Uranium there is soluble Uranium occurring in two oxidation states (U^{4+} and U^{6+}), but in most environments the soluble U^{6+} form dominates. Thorium mainly occurs in the 4+ oxidation state and is largely insoluble in natural waters. Groundwaters, rivers or seawater therefore contain considerable amounts of dissolved U but virtually no Th. In rocks of geological age ^{238}U is in activity equilibrium with its daughter nuclides including ^{234}U . However, the α -recoil effect on the α decay leads to preferential leaching of ^{234}U and hence fractionation between ^{234}U and ^{238}U in the leachate. Thus, $^{234}\text{U}/^{238}\text{U}$ isotope ratios of ground- and river-waters are usually higher than the equilibrium value. The modern $^{234}\text{U}/^{238}\text{U}$ activity ratio in marine waters is around 1.146 (Chen et al., 1986; Robinson et al., 2004).

Pore waters provide means for U transport into and out of the sediment. There are various possible scenarios such as U exchange between dissolved and particulate phase, U uptake, U loss or U mobilisation and any organic material being in exchange with the pore waters is affected by these processes. U uptake is known to be a dominant feature for organic carbonate such as mollusc shells. But sediment cement is a result of an inorganic precipitation process and thus, little can be inferred from shells about U uptake processes occurring in interstitial carbonate. The few available data, generated by us (for technical details see Appendix), are displayed in Figs 1 and 2. Fig. 1 shows concentrations of 0 ppm up to around 5 ppm in carbonate cement. In Fig. 2 the U uptake in shell and carbonate matrix is plotted against the age of the sample. It shows that with time the uptake in shell can increase (not in all samples) while there is no increase of U concentration in the matrix. This suggests that, if uptake takes place, it happens during primary cementation and not later during burial. The assumption of an inert carbonate matrix (Nathan and Mauz, 2008) is therefore contested.

We conclude from these data that gradually growing carbonate cement can contribute from nil up to several percent to the dose rate. How this gradual increase ultimately impacts on the dose rate over time depends largely on the ratio between changing U content on the one side and constant Th and K content on the other side. The more other radioactive

sources (K, Th) are part of the detrital sediment component in a sediment, the smaller will be the relative difference between onset and final dose rate (where onset dose rate represents the radiation field at the time of deposition and the final dose rate is the one of chemical stability).

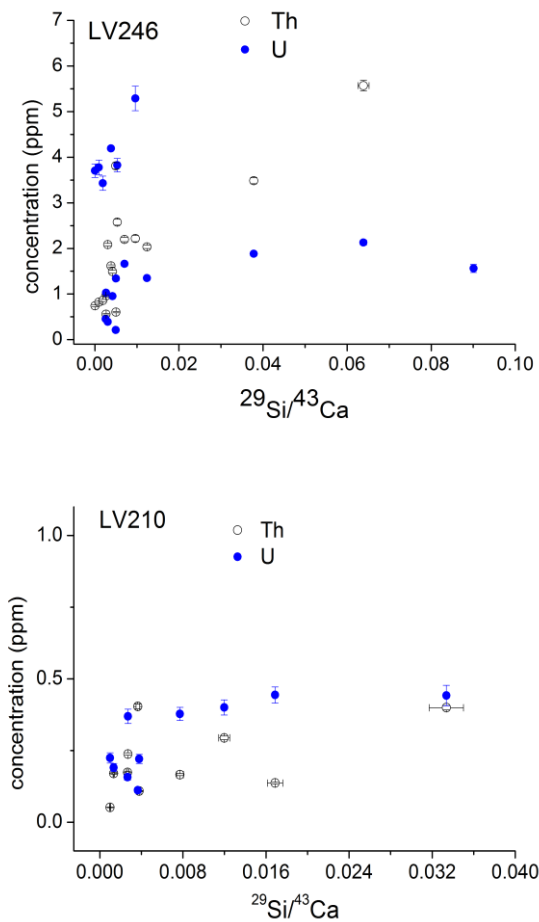


Figure 1: The concentration of U and Th in carbonate cement plotted against Si/Ca for two samples originating from different geological regions. Data with Si/Ca \sim 0.00 can be used for interpreting the activity of the carbonate component in the sample. LV246 originate from an around 6 ka old aeolian deposit on the south Adriatic coast (Italy) where the bedrock is limestone. LV210 originate from an around 57 ka old aeolian deposit on the Levant coast (Israel) where the bedrock is limestone. These data indicate a large variability of activity (0.1-5.5 ppm) of the secondary carbonate.

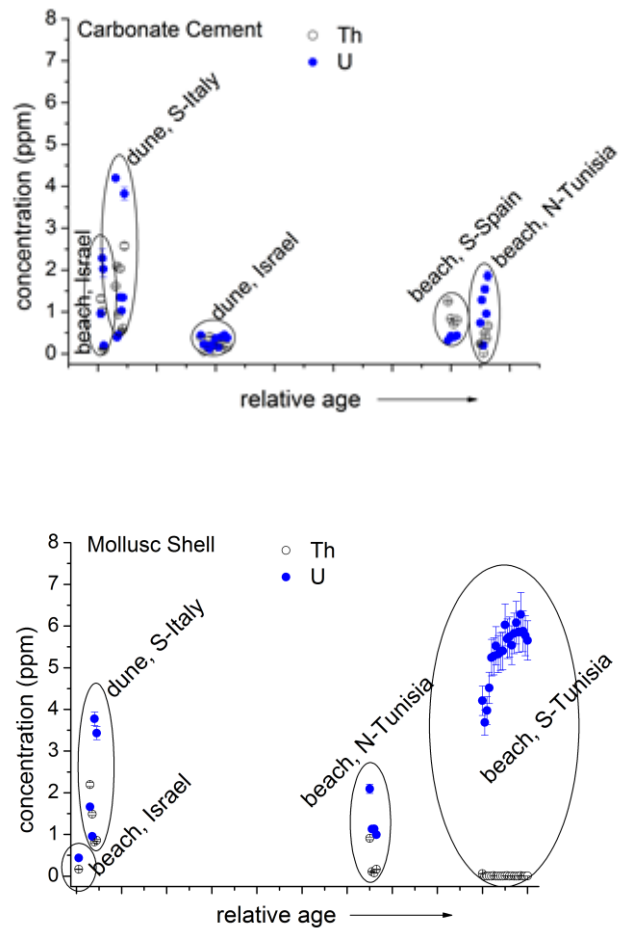


Figure 2: The concentration of U and Th in mollusc shells and carbonate cement plotted against relative age of samples. The data suggest early uptake of U in secondary carbonate whereas the uptake in mollusc shells can be continuous in time. In two samples (S-Italian dune sediment and N-Tunisian beach sediment) the U-uptake is similar in amount; in one sample (Israel beach sediment) more U is up-taken in the cement than in shells. For measurement details see Appendix.

The accurate estimation of a changing dose rate over time requires knowledge on the initial U activity ratio. In a closed system this ratio is constant and there is compelling evidence that virtually no natural carbonate environment behaves as a closed system (e.g., Thompson et al., 2003; Edwards et al., 2009). We measured shell fragments and carbonate matrix in two samples (LV111 and LV107) for their $^{230}\text{Th}/^{238}\text{U}$ and $^{234}\text{U}/^{238}\text{U}$ ratios (for technical details see Appendix). The $^{230}\text{Th}/^{238}\text{U}$ ratio allowed calculating an apparent age from which the apparent initial $^{234}\text{U}/^{238}\text{U}$ can be deduced (Fig. 3). For LV111, both

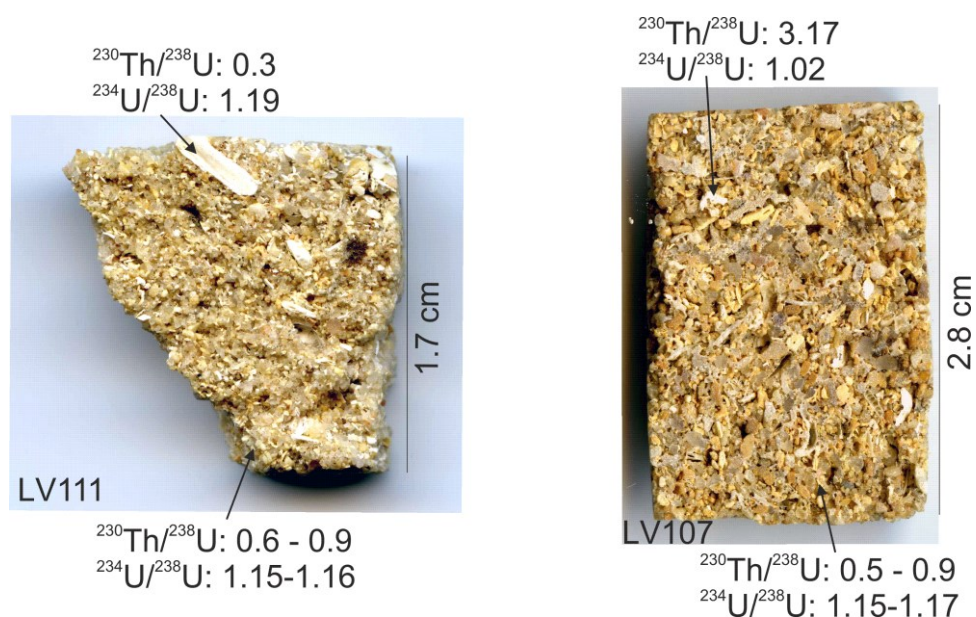


Figure 3: The activity ratios in samples LV111 and LV107. For data see Table 2. The upper arrows in each photo indicate the shell, the lower arrows the cement matrix.

shell and carbonate matrix have mean measured $^{234}\text{U}/^{238}\text{U}$ activities that are greater than the marine value of 1.146. But with the large uncertainty associated with laser ablation $^{234}\text{U}/^{238}\text{U}$ isotope ratio measurements, the measured ratios for matrix actually overlap with the marine value. The shell of

LV111 has a measured $^{234}\text{U}/^{238}\text{U}$ activity of 1.19 and an apparent initial $^{234}\text{U}/^{238}\text{U}$ activity of 1.21 indicating an open system. Assuming an initial marine signature for the matrix, the measured

ID	$^{230}\text{Th}/^{238}\text{U}$	\pm	$^{234}\text{U}/^{238}\text{U}$	\pm	Age (ka)	\pm	Initial $^{234}\text{U}/^{238}\text{U}$	\pm
LV111-shell	0.3030	0.010	1.1915	0.010	31.8	1.19	1.210	0.011
LV111-matrix1	0.9093	0.043	1.1641	0.019	156.0	16.69	1.255	0.027
LV111-matrix2	0.5612	0.030	1.1589	0.024	71.0	5.68	1.194	0.028
LV107-matrix1	0.5415	0.059	1.1452	0.036	68.8	10.84	1.176	0.043
LV107-matrix2	0.8896	0.051	1.1704	0.022	147.2	18.19	1.258	0.031
LV107-shell	3.1654	0.095	1.0248	0.023	-	-	-	-

Table 2: The activity ratios in samples LV111 and LV107 and their related uncertainties. Analytical errors are at 95 % confidence level. Age (ka) refers to the apparent U/Th age of the relevant material measured and does not represent the depositional age of the sample. For calculation of those values the reader is referred to the Appendix.

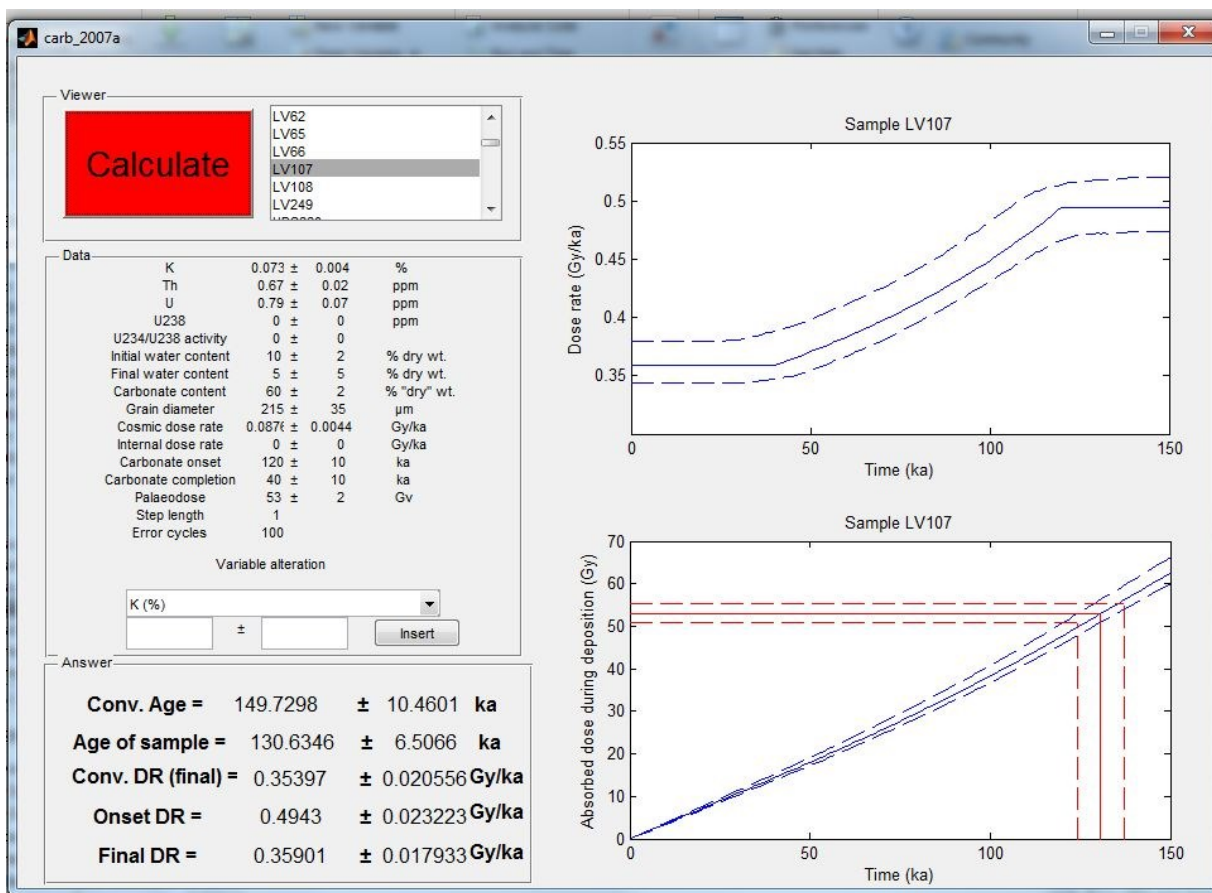


Figure 4: The upper graph shows the dose rate over time (solid blue line) with 95% confidence interval (dashed blue line). The water content is reduced proportionately to the accumulation of carbonate in the sediment pores until it reaches a new constant level. The lower graph shows the increase in absorbed dose over time (blue solid line) with 95% confidence interval (dashed blue line) as a function of the integrated dose rate. The age of the sample is estimated by projecting the D_e (red line) and the error onto the dose function.

$^{234}\text{U}/^{238}\text{U}$ activity ratios of 1.159 and 1.164 and the apparent initial $^{234}\text{U}/^{238}\text{U}$ activity ratios of 1.19 and 1.26 also indicate an open system for the matrix. The shell of LV107 has a measured $^{234}\text{U}/^{238}\text{U}$ activity of 1.02. Here, the measured $^{230}\text{Th}/^{238}\text{U}$ activity ratio of 3.17 is in excess of natural activity ratios and suggests U loss for this sample, probably after initial U uptake into the shell. No initial $^{234}\text{U}/^{238}\text{U}$ ratio can be calculated for this shell. The matrix has measured $^{234}\text{U}/^{238}\text{U}$ activity ratios of 1.145 and 1.17 and the apparent initial $^{234}\text{U}/^{238}\text{U}$ activity ratios of 1.176 and 1.258 also indicate an open system for this matrix (for data see Table 2 and Fig. 3).

These data confirm the open system behaviour of samples that contain inorganic (cement) and organic (shell) carbonate. To date, the impact of the activity ratio on the dose rate is unknown.

Description of the code

Carb accounts for the post-depositional chemical alteration of the sediment caused by cementation and for post-mortem Uranium uptake in mollusk shells. The dose rate over time is constructed as a series of values (Fig. 4) where the water content is reduced proportionately to the accumulation of carbonate in the sediment pores until it reaches a new constant level. The age of the sample is estimated as the length of time needed for the integrated dose rate to equal the equivalent dose (D_e). Uncertainties in the dose rate and ages are estimated using a Monte-Carlo approach.

Carb is written for the MATLAB software. The MATLAB script is called *Carb.m* and the input file is *SAMPLE_DATA.txt*. The script contains all necessary steps to build the dose-rate model based on the data provided in the input file.

After loading the two files into the workspace of MATLAB and running the script, the command surface appears (Fig. 4). Here, the user selects the sample. The input values of the selected sample appear below the calculate button. These can be modified using the 'Variable Alternation' option by selecting the variable, type the new value, click insert and then calculate. The script provides 5 answers: (1) the conventional age based on the conventional dose rate, (2) the conventional dose rate, (3) the age of the sample as modelled by *Carb*, (4) the dose rate before secondary carbonate started forming (onset) and (5) the final dose rate (Fig. 4). The final dose rate and the conventional dose rate must agree within 1.5%.

Data and data input

Data required are: K, Th, U, ^{238}U , $^{234}\text{U}/^{238}\text{U}$, water content initial and final, carbonate content, grain diameter, cosmic dose rate, internal dose rate, onset and termination of carbonate formation, De, step size, error cycle (i.e. the number of Monte Carlo iterations). For units of the input data see Fig. 4. Most of these data are required for conventional dose-rate estimation and the reader is referred to Aitken (1985) for details. ^{238}U is the initial detrital U before secondary carbonate started forming. ^{238}U and the U-activity ratio is ideally determined by relevant techniques (e.g. ICP-MS) or taken from literature (Chen et al., 1986; Gascoyne, 1992) or inferred from the U/Th ratio (see Ivanovich and Harmon, 1992 for the U/Th ratio in the upper earth crust).

Data input is managed through the file SAMPLE_DATA.txt. The input file has the format

LV111	LV107
0.105	0.073
0.004	0.004
0.650	0.670
0.002	0.020
1.250	0.790
0.080	0.070

where each column represents the data of one sample and the values of each row are followed in the subsequent row by their respective error values. For order of data see also Fig. 4.

Underlying assumptions of the code

The code is based on the following assumptions which are be discussed below: (1) the carbonate content is secondary carbonate resulting from the cementation process; (2) the growth of carbonate cement is linear and it is inversely correlated with the moisture content; (3) water and carbonate are inert and therefore the number of decays within a unit volume is constant; (4) U uptake by biological

remains and initial U-activity ratio is known; (5) there is no migration of radioisotopes within the sediment; (6) the sediment is homogeneous at any particular time and (7) the ionising radiation is in charged particle equilibrium.

Assumption (2) is relatively robust because the deviation from linearity is small over time. Assuming constant number of decays per unit volume of sediment (ass. 3) and absence of radioisotope migration (besides U-uptake; ass. 5) is more problematic. The series of constructed values as shown in Fig. 4 is in nature more variable between the onset and termination of dose-rate change. Also, the equilibrium of the charged-particle fluence is only an approximation for sedimentary environments because spatial variation of the fluence is a function of particle size and pore-size distribution as well as lithic and pore-size structures (e.g., Guérin et al., 2012).

Discussion

The purpose of this section is to discuss and highlight important aspects and questions of dose-rate modelling for carbonate rich samples.

The timing of cementation during burial:

Petrographic analyses allow distinguishing between early and late cementation and thereby approximating the timing of onset and termination. In addition, *Carb* allows testing different scenarios. Moreover, Nathan and Mauz (2008) showed that *Carb* is relatively insensitive to the timing of the carbonate ingrowth. In other words, the lack of the ability to quantify onset and termination of cementation has a minor impact on the accuracy of the model output.

Instantaneous cementation: If the cement formation is instantaneous, the change of dose rate over time may indeed be negligible. However, instantaneous cementation is very rare in nature (Morse and Mackenzie, 1990) and the assumption would require evidence through petrographic analysis.

The change of dose rate over time in cemented sediments:

Secondary carbonate, which has energy absorption coefficients that differ from air or water, precipitates in the pore space over time and not at once. The exact time span is hard to determine because sediment carbonate geochemistry is a function of thermodynamics, dissolution and precipitation kinetics and surface chemistry of carbonate minerals. From a conceptional point of view we can say that for any given late Quaternary sediment it may take 10^2 - 10^5 years to reach chemical stability. While the 10^2 years timescale is well known in carbonate sedimentology (e.g. Morse and Mackenzie, 1990) because it is an interesting

exception in nature, the 10^5 years timescale is used here by the author to illustrate that chemical stability may not be reached over the time span covered by the dosimeter.

Does the carbonate content impact on the dispersion of D_e values? The answer to this question requires comparison of the radioactivities of matrix (carbonate) and primary detrital components where the latter potentially hosts a radioactive hotspot. Likewise, it requires simulation work. In the absence of this work a brief estimation can be made: The range of 1 MeV electrons is in water twice as large as it is in carbonates. As a result, radiation from hotspots would reach a smaller volume of detrital components when carbonate covers the pore space instead of water or air. Taking the results of Mayya et al. (2006) into account, it is likely that the dispersion of D_e values increase with increasing carbonate content.

Daylight bleaching and carbonate ingrowth: The deposition of the dosimeter as part of the detrital component of the sediment occurs prior to cementation and there are several orders of magnitude time difference between bleaching and (instantaneous) cementation.

Detrital versus secondary carbonate: The differentiation and quantification of detrital versus secondary carbonate requires petrographic analysis. If the detrital component is dominant, i.e. if the sample is barely cemented, the change of dose rate over time is negligible. Detrital carbonate originating from limestone bedrock is mostly inert and contributes to the heterogeneity of the beta radiation field in the sample. Typically, the size of the limestone particles is different from that of the other primary sediment components due to different material properties. In this case the carbonate element creates a geometry issue of the infinite matrix concept, which is discussed by Guérin et al. (2012).

Secondary carbonate and water: Based on fundamental principles and empirical evidence in sedimentology, it is expected that the texture of the sediment (e.g. packing of components) does not change during the cementation process and *Carb* therefore assumes that the carbonate cement is inversely correlated with the moisture content. Thus, during burial the total volume of the sediment remains approximately the same, while density and mass change.

By how much does the dose rate change due to secondary carbonate? If, for example, 40% carbonate matrix was precipitated syn-sedimentarily,

the change of dose rate over time would be negligible. The correction factor would be different but this difference would be small. It is the interplay between all parameters that affects the accuracy of the age estimate and this cannot be assessed by examining parameters individually.

Does the ingrowth of secondary carbonate result in age underestimation? The carbonate infill has different dose-deposition efficiencies, which can result in both under- and overestimation of age if this efficiency is not taken into account. Nathan and Mauz (2008) and Mauz et al. (2009) show however, that dose-rate modelling using *Carb* results in lower ages compared to a steady state dose-rate estimation. The lower ages are a consequence of the lower dose-deposition efficiency of carbonate compared to water under the assumption that the carbonate matrix is inert. But even if the carbonate matrix is not inert, the data plotted in Figs 1, 2 and 3 suggest that a decrease of dose rate during burial is more likely than an increase. The rationale here is that the data (Fig. 2) indicate an early uptake of U in the carbonate matrix while the absorption of radiation through carbonate is continuous throughout the time of burial and more effective than through water. When plotting dose rate against burial time (Fig. 4), the slope of the curve would probably be less steep for a sample with an active carbonate matrix compared to a sample with an inert matrix.

Field appearance of cemented sediment deposits: Well-preserved beds of a cemented sediment deposit are those with a spatially relatively constant cement to porosity ratio and are therefore the preferred sampling target.

Carb and petrographic analyses: Although beneficial, *Carb* does not require petrographic analyses. It requires quantification of the carbonate content, which is a straightforward laboratory analysis.

Carbonate ingrowth and the contribution of U to the dose rate: In general, the contribution of U to the effective dose rate is small if the sample is from a closed sedimentary system. While U can create secular disequilibrium in the sediment, for cemented samples it is the energy absorption efficiencies of different materials for beta and gamma radiation originating from K, Th and U that are important.

Can the modern marine U activity ratio be adopted for all cemented samples? In theory not, because the carbonate cement could have precipitated from meteoric water with a very different initial activity ratio. In practice, the impact of an inaccurate activity

ratio on the dose rate is probably small unless U is the only radioactive source in the sediment.

Final remarks

In most carbonate-rich samples the dose rate generated by external alpha, beta and gamma radiation is low (e.g. <1 Gy/ka) to very low (e.g. 0.3 Gy/ka). A low external dose rate raises the importance of the internal (i.e. within the dosimeter) and the cosmic dose rate.

The application of the model does not require detailed understanding of the underlying physics, carbonate geochemistry or MATLAB software.

The robustness of the algorithm is limited. Extreme sample values cannot be handled. Thus, the sample must conform to the carbonate dose-rate model and its assumptions as described above. Adjusting parameters is an advantage of the code, but this option is probably restricted to users with expert knowledge.

The script file, a template file for the data input and further instructions can be downloaded from the Ancient TL webpage.

Acknowledgements

We are grateful for the input of the two reviewers Guillaume Guerin and Ashok Singhvi. We also thank the editor for her thoughtful comments.

References

- Aitken, M.J., 1985. Thermoluminescence Dating. Academic Press, London, 378pp.
- Aitken, M.J., Xie, J., 1990. Moisture correction for annual gamma dose. *Ancient TL* 8, 6–9.
- Chen, J.H., Edwards, R.L. and Wasserburg, G.J., 1986. ^{238}U - ^{234}U - ^{232}Th in seawater. *Earth and Planetary Science Letters*, 80, 241-251.
- Edwards, R.L., Gallup, C.D. and Cheng, H. Uranium-series dating of marine and lacustrine carbonates. In: Bourdon, B., Henderson, G.M., Lundstrom, C.C. and Turner, S.P. (eds), *Uranium-series geochemistry. Reviews in Mineralogy & Geochemistry* 52, 363-405pp.
- Gascoyne, M., 1992. Geochemistry of the actinides and their daughters. In: Ivanovich, M., Harmon, R.S. (Eds.), *Uranium-series Disequilibrium: Applications to Earth, Marine, and Environmental Sciences*, pp. 34-61.
- Guérin, G., Mercier, N., Nathan, R., Adamiec, G. and Lafrays, Y., 2012. On the use of the infinite matrix assumption and associated concepts: A critical review. *Radiation Measurements* 47, 778-785.
- Guérin, G. and Mercier, N., 2012. Preliminary insight into dose deposition processes in sedimentary

- media on a scale of single grains: Monte Carlo modelling of the effect of water on the gamma dose rate. *Radiation Measurements* 47, 541-547.
- Hoffman, D.L., Spötl, C. and Mangini, A., 2009. Micromill an in situ laser ablation sampling techniques for high spatial resolution MC-ICPMS U-Th dating of carbonates. *Chemical Geology* 259, 253-261.
- Ivanovich, M., Harmon, R.S., 1992. Uranium-series disequilibrium: Applications to Earth, Marine, and Environmental Sciences.
- Mauz, B., Fanelli, F., Elmejdoub, N., Barbieri, R., 2012. Coastal response to climate change: Mediterranean shorelines during the last interglacial (MIS 5). *Quaternary Science Reviews* 54, 89–98.
- Mauz, B., Hijma, M.P., Amorosi, A., Porat, N., Galili, E., Bloemendal, J., 2013. Aeolian beach ridges and their significance for climate and sea level: concept and insight from the Levant coast (East Mediterranean). *Earth Science Reviews* 121, 31–54.
- Mauz, B., Elmejdoub, N., Nathan, R.P. and Jedoui, Y., 2009. Last interglacial coastal environments in the Mediterranean–Saharan transition zone. *Palaeogeography, Palaeoclimatology, Palaeoecology* 279, 137–146.
- Mayya, Y.S., Morthekai, P., Murari, M.K. and Singhvi, A.K., 2006. Towards quantifying beta microdosimetric effects in single-grain quartz dose distribution. *Radiation Measurements* 41, 1032-1039.
- Nathan, R.P. and Mauz, B., 2008. On the dose-rate estimate of carbonate-rich sediments for trapped charge dating. *Radiation Measurements* 43, 14-25.
- Morse, J.W. and Mackenzie, F.T., 1990. Geochemistry of sedimentary carbonates. *Developments in Sedimentology* 48. Elsevier, 707p.
- Robinson, L.F., Belshaw, N. and Henderson, G.M., 2004. U and Th concentrations and isotope ratios in modern carbonates and waters from the Bahamas. *Geochimica et Cosmochimica Acta*, 68, 1777-1789.
- Thompson, W.G., Spiegelmann, M.W., Goldstein, S.L., Speed, R.C., 2003. An open-system model for U-series age determinations of fossil corals. *Earth and Planetary Science Letters* 210, 365–381.
- Zimmerman, D.W., 1971. Thermoluminescence dating using fine grains from pottery. *Archaeometry* 13, 29–52.

Reviewer

G. Guerin, A. Singhvi

Appendix

Measuring the Uranium and Thorium element concentrations (Figures 1 and 2):

Aa New Wave UP193HE laser coupled to a Thermo Element 2 sector field ICPMS was used. The laser was operated at a repetition rate of 5 Hz, a spot diameter of 30 μm and an energy density of 4-5 J/cm^2 . The counting time for a single analysis was 120 s with 60 s measuring gas blank to establish the background count rates and 60 s for laser ablation. The following isotopes were used for elemental analysis: ^{29}Si , ^{43}Ca , ^{44}Ca , ^{232}Th and ^{238}U . Total dwelling time on each peak was 60 ms. The NIST 610 glass standard was used for calibrating the relative element sensitivities. The concentrations were taken from Pearce et al. (1997). The CaO concentration of the carbonate samples was assumed to be 55 wt %. With a laser penetration depth of 30-50 μm and a laser spot size of 30 μm^2 , the purity of the spot in terms of "carbonate only" was ascertained by plotting the data of each spot against their Si/Ca ratio (Figs 1 and 2) where Si/Ca ~ 0 indicates pure carbonate.

Measuring the activity of inorganic (pore material) and organic (shell) carbonate (Figure 3):

The samples were analysed using laser ablation (LA) multi-collector (MC) - inductively coupled mass spectrometry (ICPMS) U-Th disequilibrium techniques following the method outlined by Hoffmann et al. (2009). All MC-ICPMS measurements were performed using a ThermoFinnigan Neptune coupled with a New Wave Research UP193HE ArF Excimer laser system. Samples were placed in a laser sample cell together with an in-house carbonate U-Th LA calibration sample, which is a secular equilibrium calcite 'standard' for correction of instrumental biases of LA U-Th isotope measurements on CaCO_3 . Ablation is done using He as carrier gas which is mixed with Ar sample gas and N_2 in a quartz mixing cell before injection into the Ar plasma. Typical laser power density is 5 J/cm^2 at 70 % power output, for U-Th isotope LA measurements presented in this study we used 7 Hz repetition rate and a 90 μm diameter spot size. A LA measurement was done on a 0.5 mm long track, ablated by moving the laser spot at a speed of 20 $\mu\text{m}/\text{s}$ along the track in 6 passes. A standard - sample - standard bracketing procedure was applied and data collection and corrections were carried out following Hoffmann et al. (2009).

Calculation of age and apparent initial $^{234}\text{U}/^{238}\text{U}$ ratios (Table 2):

$^{230}\text{Th}/^{238}\text{U}$ and $^{234}\text{U}/^{238}\text{U}$ at the present time t were measured. The following equation is used to (iteratively) calculate the age t :

$$\left(\frac{^{230}\text{Th}}{^{238}\text{U}}\right)(t) = (1 - e^{-\lambda_{230} t}) + \left(\left(\frac{^{234}\text{U}}{^{238}\text{U}}\right)(t) - 1\right) \frac{\lambda_{230}}{\lambda_{230} - \lambda_{234}} (1 - e^{-(\lambda_{230} - \lambda_{234}) t})$$

Decay constants λ are $9.1577 \times 10^{-6} \text{ a}^{-1}$ for ^{230}Th , $2.826 \times 10^{-6} \text{ a}^{-1}$ for ^{234}U , $1.55125 \times 10^{-10} \text{ a}^{-1}$ for ^{238}U . Using the calculated age t , the apparent initial ratio $^{234}\text{U}/^{238}\text{U}$ follows from

$$\left(\frac{^{234}\text{U}}{^{238}\text{U}}\right)(t) = \left(\left(\frac{^{234}\text{U}}{^{238}\text{U}}\right)_{\text{init.}} - 1\right) e^{-\lambda_{234} t} + 1$$